THE ASTROPHYSICAL JOURNAL, 404:219–231, 1993 February 10

158 MICRON [C II] MAPPING OF THE ORION MOLECULAR CLOUD

G. J. STACEY,[1] D. T. JAFFE,[2] N. GEIS,[3] R. GENZEL,[4] A. I. HARRIS,[4]
A. POGLITSCH,[4] J. STUTZKI,[5] AND C. H. TOWNES[3]
Received 1992 March 23; accepted 1992 August 10

ABSTRACT

We have constructed a fully sampled, 1000 point, 1′ resolution map of the inner 6′.5 × 10′($\alpha \times \delta$) regions of the Orion Nebula in the 157.7409 μm [C II] fine-structure line. We have also obtained large-scale ($\sim 1°$) strip maps in [C II] across the face of the Orion molecular cloud, and CO(17–16), (14–13), and (7–6) spectra at selected positions in the Orion H II region/molecular cloud interface.

Within $\sim 2'.5$ of Θ^1 Ori C (hereafter, the interface region) the [C II] line emission arises in warm ($T \sim 300$ K), dense ($n_H \sim 4 \times 10^5$ cm^{-3}), photodissociated gas at the interface between the H II region and the molecular cloud. The photodissociated gas represents $\sim 3\%$ of the total gas mass toward the interface region of the Orion molecular cloud. The [C II] intensity distribution is similar to that of CO(1–0) and (7–6). Furthermore, for the interface region, the CO(7–6) and [C II] spectral profiles are similar, indicating that both submillimeter and millimeter CO lines originate from the UV-heated warm quiescent gas in the interface region. The distribution of CO intensity with rotational quantum number indicates that this CO-emitting gas is warm, $T_{gas} \sim 140$ K, and dense, $n_{H_2} \sim 1.4 \times 10^4$ cm^{-3}. This warm CO component is a large fraction ($\sim 35\%$) of the total molecular gas mass in the interface region. Current photodissociation region models fail to explain the large column densities of warm CO.

Strong [C II] line emission is observed across the face of the Orion molecular. We estimate the total [C II] luminosity from the Orion molecular cloud is $\sim 1500\ L_\odot$ or 0.3% of the far-infrared luminosity. The extended [C II] emission probably arises from either the UV-exposed surface of the molecular cloud or from the surfaces of UV-exposed clumps within the molecular cloud. The source of the far-ultraviolet (FUV) radiation is likely the Trapezium cluster. A simple model is presented which matches the observed [C II] intensity distribution by invoking a clumpy rim of intervening gas between the Orion H II region and the outer regions of the Orion molecular cloud. FUV flux from the Trapezium penetrates this rim and falls on the outer regions of the molecular cloud, thereby giving rise to the relatively flat distribution of [C II] emission we observe. Alternatively, the FUV source for the extended [C II] emission may be the ambient interstellar radiation field if that field is ~ 25 times the local interstellar radiation field, or embedded FUV sources in the molecular cloud. The mass contained in these extended photodissociation regions is $\sim 3\%$ of the molecular mass of the Orion molecular cloud. The extended [C II] distribution is similar to that of the [C I] 610 μm fine-structure line. It is therefore likely that the [C I] emission also arises from these extended photodissociation regions in molecular clouds.

The overall properties of the Orion molecular cloud deduced through our measurements including the photodissociated gas to molecular gas mass fraction, the [C II] line to far-infrared continuum intensity ratio, and the [C II]/^{12}CO(1–0) line intensity ratio are the same for the Orion molecular cloud and the nuclei of nonstarburst galaxies. Hence the molecular medium in nonstarburst nuclei may be constructed through a superposition of Orion-like molecular clouds. These observations therefore provide an important link between [C II] emission from Galactic molecular clouds and the nuclei of external galaxies.

Subject headings: H II regions — ISM: clouds — ISM: individual (Orion Nebula) — ISM: molecules

1. INTRODUCTION

The $^2P_{3/2}$–$^2P_{1/2}$ (157.7409 μm) fine-structure line of C^+ has been detected from a wide variety of Galactic and extragalactic sources including regions as diverse as planetary nebulae and distant *IRAS* galaxies (e.g., Crawford et al. 1985; Stacey et al. 1991a, and references therein). The [C II] line emission from these sources primarily arises in warm ($T_g \gtrsim 200$ K), dense ($n_H \gtrsim 10^3$ cm^{-3}) photodissociated gas regions at the surfaces of giant molecular clouds (GMCs) exposed to ionizing FUV radiation. The photodissociated gas is heated both by the photoelectric ejection of energetic electrons from grains and, in high-density gas regions, through the collisional de-excitation of FUV-pumped vibrationally excited molecular hydrogen. The primary gas-cooling mechanism is collisionally excited fine-structure-line radiation of C^+, O^0, and Si^+ (cf. Tielens & Hollenbach 1985a; Sternberg & Dalgarno 1989; van Dishoeck & Black 1988).

The nearby ($d \sim 480$ pc; Genzel et al. 1981) Orion star formation complex is a primary source for the study of photodissociation regions (PDRs). Initial studies of this region in the 158 μm [C II], and 63 and 145 μm [O I] fine-structure lines indicated that the photodissociated gas near the Orion H II region/GMC interface region has densities $\sim 2 \times 10^5$ cm^{-3} and temperatures ~ 350 K (Stacey et al. 1983; Stacey 1985;

[1] Department of Astronomy, Cornell University, Ithaca, NY 14853.
[2] Department of Astronomy, R. L. Moore Hall, University of Texas, Austin, TX 78712.
[3] Department of Physics, University of California, Berkeley, CA 94720.
[4] Max-Planck-Institut für extraterrestrische Physik, W-8046 Garching, Germany.
[5] I. Physikalisches Institut, Universität Köln, Zülpicherstr. 77, W-5000 Köln 41, Germany.

Tielens & Hollenbach 1985b). These low-resolution studies (beam $\sim 4' \times 7'$) leave several important questions unanswered. What is the detailed morphology of the Orion photodissociation region and what is its relationship to the Orion molecular cloud? In particular, what is the effect of the UV flux from the nearby OB cluster on the molecular gas at the surface of the molecular cloud? The large-scale measurements of [C II] radiation from other molecular clouds (e.g., M17, NGC 2024, W3, NGC 1977, and NGC 2023; Russell et al. 1981; Kurtz et al. 1983; Melnick et al. 1986; Stutzki et al. 1988; Matsuhara et al. 1989; Howe et al. 1991) indicate that molecular clouds are clumpy, allowing penetration of carbon-ionizing photons to parsec depths. Alternatively, if the [C II] radiation arises from the surfaces of molecular clouds, these surfaces must be exposed to FUV radiation fields several times the local interstellar radiation field (ISRF). Is there evidence for wide-scale [C II] radiation from the Orion molecular cloud? What is the connection between this large-scale [C II] emission and the integrated [C II] emission from the Galaxy (Stacey et al. 1985; Shibai et al. 1991; Wright et al. 1991) and the bright [C II] lines observed from external galaxies (Crawford et al. 1985; Stacey et al. 1991a)?

To address these questions, we undertook a multiwavelength study of the Orion molecular cloud. We present the first fully sampled 1′ resolution map of the [C II] line emission from the inner $7'(\alpha) \times 10'(\delta)$ region of Orion A, plus two strip maps ($\sim 1°$ extent) of the [C II] line emission across the face of the Orion molecular cloud. We also report measurements of the CO(7–6), (14–13), and (17–16) rotational transitions toward selected positions in the Orion interface region.

2. OBSERVATIONS

2.1. [C II] *Observations*

The [C II] observations were taken with the (Mk II) high spectral resolution UC Berkeley tandem Fabry-Perot spectrometer (Lugten 1987) during a KAO flight on 1988 January 12. This was the first flight with a new three element stressed Ge:Ga detector array (Stacey et al. 1991a). This array allows simultaneous mapping at three positions separated by 55″ at a position angle determined by the rotation angle of the source at the time of observations. The data were taken with a 55″ (FWHM) beam ($\Omega = 8.6 \times 10^{-8}$ sr), at a spectral resolution of 67 km s^{-1} (FWHM). The [C II] line is not spectrally resolved. The system noise equivalent power (NEP) including all losses was ~ 3 and 4×10^{-15} W Hz$^{-1/2}$ for the central and side detectors, respectively. Line intensity calibration (accuracy $\pm 30\%$) was made through continuum observations of Jupiter which was assumed to emit like a 127 K blackbody (Hildebrand et al. 1985).

2.1.1. *Orion Interface Region Map*

We obtained a fully sampled, two-dimensional [C II] map of the Orion interface region. First, the frequency scale was established by scanning the Fabry-Perot filter across the [C II] line toward Θ^1 Ori C. Then, the scanning Fabry-Perot was fixed at the [C II] line frequency, and the telescope beam was rastered across the source. The maps we acquired are therefore [C II] line plus 158 μm continuum maps. The continuum represents a small correction ($\sim 10\%$) except for the regions within $\sim 1'$ of the BN-KL nebula. All of the raster observations were single beam observations, that is, we chopped the KAO secondary in the standard manner, but we did not beam switch (nod) the telescope. The chopper throw was 5′.8 east-west, with the reference beam to the west of the signal beam. The raster map pattern was a rectangular $11(\alpha) \times 6(\delta)$ step grid with a 30″ space between grid steps. Each individual raster map is therefore fully sampled by the central detector and covers a $5'(\alpha) \times 2'.5(\delta)$ region. The side detectors, located 55″ away from the central detector at position angle $\sim 115°$ ($\Delta\alpha = \pm 50''$, $\Delta\delta = \mp 23''$), thus served to extend the map borders and increase the signal-to-noise ratio and sampling in the inner regions. Including the data from the side detectors, the east-west extent of the map is 6′.7, so that the easternmost arcminute of the map was obtained with the reference beam on the westernmost arcminute of the map. However, the [C II] emission from the easternmost regions is significantly (factor of 3) stronger than that from the westernmost regions of the map (see § 3.1), so that these contours are largely unaffected by emission in the reference beam. This effect is at the level of 5% of the peak [C II] intensity.

Four line + continuum maps were made: one centered on Θ^1 Ori C ($\alpha_{1950} = 5^h32^m49^s.0$, $\delta_{1950} = -5°25'16''$) one each centered at 2′.5 north and south of Θ^1 Ori C, and one 5′ south of Θ^1 Ori C. In addition, we also made one map of the continuum (6′.7[α] × 3′.3[δ], including side channels) centered on Θ^1 Ori C, where the continuum was sampled at a wavelength ~ 2.5 resolution elements (170 km s^{-1}) shortward of the [C II] line. Integration time was typically 3 s per point. The total mapping project, consisting of nearly 1000 data points (5 raster maps × 3 detectors × 66 points per map), took about 20 minutes of integration time.

2.1.2. *Orion Molecular Cloud Scan*

We also obtained two strip maps of the [C II] line radiation across the Orion molecular cloud in right ascension. These strip maps were constructed by "walking" the beams across the source (cf. Stacey et al. 1985). First the reference beam is placed in a region assumed be devoid of [C II] line emission. The first spectral scan is taken here. For the next spectral scan, the beams are moved so that the source beam is one chopper throw (5′) closer to the source, and the reference beam falls on the position of the previous source beam. The process is continued until the beams are walked across the source to a region which may again be safely assumed to be free of line emission. The result of this process is the derivative of the [C II] line emission across the source, which is integrated to derive the source line distribution. We obtained two such strip maps. For both strips, we scanned spectrally 330 km s^{-1} (4.9 resolution elements) centered on the [C II] line. We therefore determine both a "continuum," which consists of both source and telescope continuum, and a line flux. The integration time at each position varied from 1 to 5 minutes depending on the observed line strength. The total integration time on source for both strip maps was 50 minutes. The first map began with the reference beam 20′ to the west of BN-KL ($\alpha_{1950} = 5^h32^m46^s.7$, $\delta_{1950} = -5°24'17''$) and proceeded in 5′ steps to a region 30′ to the east of BN-KL. This scan passed through the central region of the nebula $\sim 15''$ north of BN-KL. The second map began with the source beam 32′.5 to the east of BN-KL and proceeded westward until the reference beam was 22′.5 to the west of BN-KL. This cut passed through the central region $\sim 90''$ north of BN-KL. At the time of the observations, the rotation angle of Orion was such that the side detectors were located at a position angle of 104° ($\Delta\alpha = \pm 53''$, $\Delta\delta = \mp 13''$) with respect to the central detector and therefore swept out nearly the same paths in right ascension.

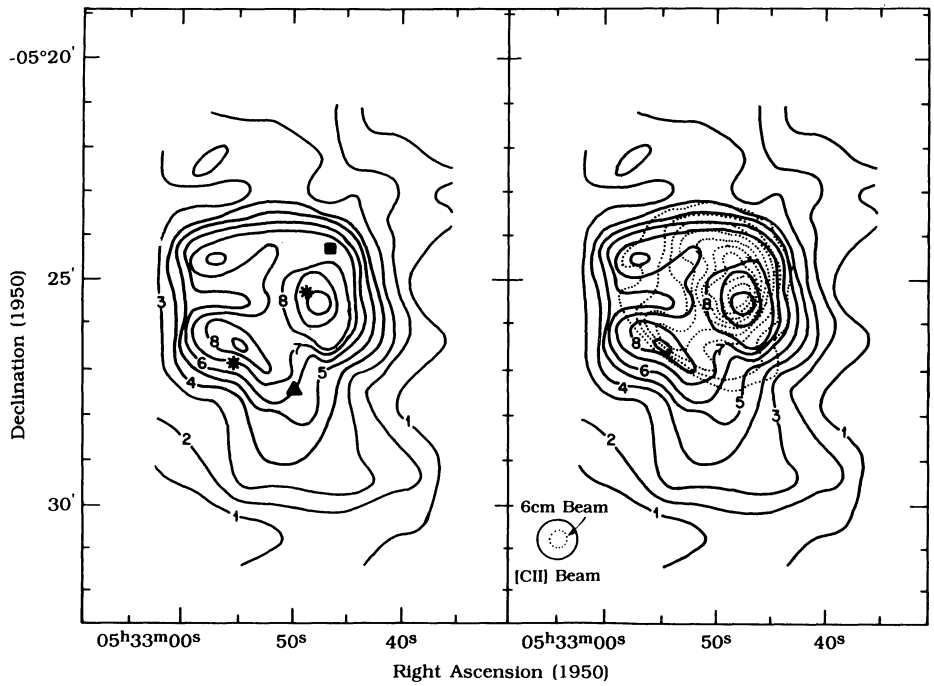

FIG. 1.—(*left*) Fully sampled [C II] map of the Orion H II region/GMC interface region. The map is not corrected for self-chopping. The contour units are 10% (5 σ), 20%, 30%, ... 100% of the peak intensity (3.9×10^{-3} ergs s^{-1} cm^{-2} sr^{-1}). To correct for self-chopping add $\sim 1.1 \times 10^{-3}$ ergs s^{-1} cm^{-2} sr^{-1} to each contour level. The BN-KL nebula and the "bar" position are marked by a solid square and triangle, respectively. Θ^1 Ori C (*center*) and Θ^2 Ori (*lower left*) are marked by stars. (*right*) [C II] map of Fig. 1 superposed on the 6 cm radio continuum contours of Johnston et al. (1983) (28″ beam). The radio contour intervals are 10%, 20%, 30%, ... 90% of the peak flux density (4.75 Jy beam^{-1}).

2.2. *Far-Infrared* CO *Observations*

Our Fabry-Perot interferometer was also used to observe the 14–13 (185.9996 μm) and 17–16 (153.2667 μm) rotational transitions of CO toward selected positions in the Orion interface. The CO (14–13) line was observed from both a region near Θ^1 Ori C and the bright optical "bar" ($\alpha_{1950} = 5^h32^m50^s.0$, $\delta_{1950} = -5°27'22''$) region of the Orion nebula on 1986 November 3. These positions are marked on Figure 1 (left). We used a spectral resolving power of 72 km s^{-1} and a 60″ beam ($\Omega = 1.0 \times 10^{-7}$ sr). The system NEP was $\sim 6 \times 10^{-15}$ W Hz$^{-1/2}$. We obtained a CO(17–16) spectrum on Θ^1 Ori C with the three detector version of our Fabry-Perot described above during a KAO flight on 1988 January 19 (beam 54″, $\Omega = 8.2 \times 10^{-8}$ sr). The spectral resolution was 30 km s^{-1}, at which the system NEP was 3×10^{-15} W Hz$^{-1/2}$. The data for both far-infrared (FIR) CO transitions were calibrated with respect to the continuum of BN-KL.[6]

2.3. *Submillimeter* CO *Observations*

The ^{12}CO(7–6) (806.6517 GHz, 371.650 μm) transition was observed toward Θ^1 Ori C and the Orion optical "bar" on 1988 February 3 using the UCB/MPE submillimeter Cassegrain spectrometer (Harris et al. 1987a) on the 3.8 m United Kingdom Infrared Telescope (UKIRT). The spectrometer front end is a liquid-nitrogen-cooled Schottky diode mixer in a quasi-optical corner cube mount, pumped with a laser local oscillator. The receiver noise temperature was approximately 4000 K (DSB). Our dual acousto-optical spectrometer with 1.1 GHz (410 km s^{-1}) bandwidth and 0.4 km s^{-1} velocity resolution served as the back-end spectrometer. Observations of a number of planets during several observing runs showed that the beam was well approximated by a 26″ FWHM Gaussian with a main beam efficiency of 32%. The submillimeter atmospheric transmission was 17%, determined by measuring the sky's radiation temperature and applying corrections for the amount of warm material in the beam and the transmission difference between the two sidebands (Harris 1986). The intensity scales for the spectra are Rayleigh-Jeans main beam brightness temperatures corrected for atmospheric attenuation and the main beam efficiency of 32%. Absolute intensity calibration is within $\pm 25\%$. The telescope secondary chopped E-W at 2 Hz with an amplitude of 3′. Pointing, which was established and monitored with the UKIRT's optical television guiding system, was well within $\pm 7''$.

[6] We have calibrated the FIR continuum of the BN-KL source with respect to the planets on several KAO flights. For a 45″ aperture ($\sim$60″–54″ [FWHM] beam) we find $F_{186\,\mu m} \sim 3.0 \times 10^4$ Jy ($\Omega \sim 1.0 \times 10^{-7}$ sr); $F_{158\,\mu m} \sim 4.2 \times 10^4$ Jy ($\Omega \sim 8.6 \times 10^{-8}$ sr); $F_{153\,\mu m} \sim 4.4 \times 10^4$ Jy ($\Omega \sim 8.3 \times 10^{-8}$ sr). These values are in good agreement with the photometric values given by Jaffe et al. (1984; 48″ beam).

3. RESULTS

3.1. [C II] *Line Mapping*

3.1.1. *Orion Interface Region Map*

The [C II] data from the interface maps were reduced by first constructing the individual calibrated line + continuum and continuum maps for each of the three detectors. Residual (uncanceled) signal from the warm telescope (a small effect) was measured by observing blank sky and subtracted from the maps. The various maps constructed for each of the detectors agreed very well (within $\sim 10\%$) in the regions where the maps overlap. The individual detector maps were therefore com-

bined to make a single highly sampled line + continuum map and continuum map. The continuum map obtained (6.'7[α] × 3.'3[δ]) is in excellent agreement with the 1′ resolution large-scale (5′ × 10′) 100 μm continuum map obtained by Werner (1982). We therefore incorporated the outer contours of this map into our continuum map. Figure 1 (left) shows the final [C II] map obtained by subtracting this synthesized continuum map from the line + continuum map.

The 158 μm [C II] line emission is strong and easily detected over the entire map. The peak line intensity ($I_{[C\ II]} \sim 3.9 \times 10^{-3}$ ergs s^{-1} cm^{-2} sr^{-1}) is ~20″ south west of the primary source of ionizing flux, Θ^1 Ori C. Spectral scans of the [C II] line obtained there consistently displayed ~35% stronger line emission when the reference beam was to the west than when the reference beam was to the east indicating that the eastern reference beam was not entirely clear of the source. The interface region map was therefore obtained with the reference beam to the west. If there were also line emission in the western reference position, this "self-chopping" would lower the observed peak line intensity of the interface map. Our large-scale cuts across the Orion molecular cloud (see below) indicate that we were self-chopping at the 22% level with the 5.'8 chopper throw employed for the interface map. Using this correction, the peak intensity of the interface map is 5.0×10^{-3} ergs s^{-1} cm^{-2} sr^{-1}. The average line intensity in a 8′(α) × 4′(δ) region centered on the Trapezium is 3.25×10^{-3} ergs s^{-1} cm^{-2} sr^{-1}, in very good agreement with the previous measurements of Russell et al. (1980) ($I_{[C\ II]} \sim 3.5 \times 10^{-3}$ ergs s^{-1} cm^{-2} sr^{-1}; 7′ × 4′ beam). The total [C II] luminosity integrated over the map is ~90 $L_\odot$, or ~3.0×10^{-4} of the total FIR continuum luminosity of the inner 6.'5 × 10′ region (~2.7×10^5 $L_\odot$; Werner et al. 1976; Werner 1982).

Several well-known optical features are also prominent in the [C II] map. There is enhanced [C II] emission along the ridge of the bright optical "bar" to the southeast, likely the result of limb-brightened emission in the optically thin [C II] line (Stacey et al. 1991b) due to a nearly edge-on geometry. The "dark bay" is also obvious in the [C II] map as a tongue of depressed [C II] emission to the east of the Trapezium cluster. There is a notable north-south extension in the lower contours of the map indicating that low brightness level [C II] line emission follows the Orion "ridge." Notice that there is no enhancement in the [C II] emission associated with the BN-KL outflow. This is consistent with the theoretical models which predict that little [C II] line emission is produced in shocks (Hollenbach & McKee 1989). Figure 1 (right) superposes the [C II] map on the 6 cm radio continuum image (28″ beam) of Johnston et al. (1983). The peaks in the free-free emission to the west of Θ^1 Ori C and near the optical "bar" are also prominent in the [C II] map. The [C II] emission falls off rapidly outside the H II region but still shows very strong emission in regions significantly beyond the H II region. The map is therefore consistent with the conclusion that the bulk of the measured [C II] line emission arises *outside the* H II *region* in the interface region between the fully ionized gas and the FUV exposed giant molecular cloud (Russell et al. 1980). There is also insufficient column density in the H II region to account for the observed [C II] intensity (Russell et al. 1980).

The [C II] line width is ~5.0 km s^{-1} (FWHM) near Θ^1 Ori C (Boreiko, Betz, & Zmuidzinas 1988). The peak line intensity ($I_{[C\ II]} \sim 5.0 \times 10^{-3}$ ergs s^{-1} cm^{-2} sr^{-1}) corresponds to a Planck-corrected main beam brightness temperature $T_P \sim 185$ K for the [C II] line. This represents the minimum gas kinetic

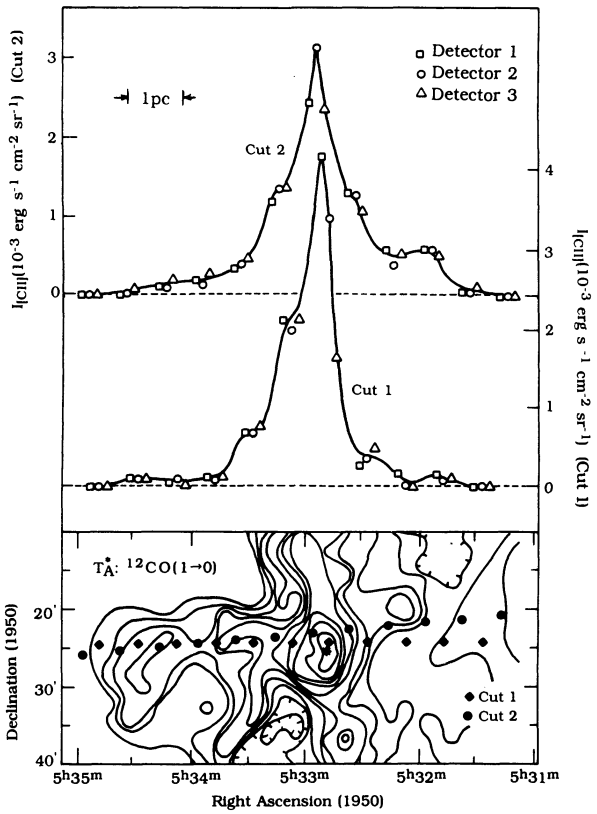

FIG. 2.—(*top*) Reconstructed [C II] strip maps across the face of the Orion molecular cloud. The peak line entensity of cut 1 is 4.1×10^{-3} ergs s^{-1} cm^{-2} sr^{-1}. Errors propagate inward from the outer regions of the strip maps where the 1 σ errors are ~3.5×10^{-5} ergs s^{-1} cm^{-2} sr^{-1} (~1% of the peak intensity). (*bottom*) Path of the two cuts superposed on the ^{12}CO(1–0) contours (2.'3 beam) of Schloerb & Loren (1982). Cut 1 passed 15″ north of BN-KL along a position angle of 90°.5. Cut 2 passed 90″ north of BN-KL along P.A. 105°. The contour unit for the CO map is $T_A^* = 5$ K, and the first contour is $T_A^* = 10$ K.

temperature of the emitting medium, appropriate in the limit of optically thick emission from a thermalized medium of unit beam filling factor. The actual gas temperature must be in excess of this value. At the position of Θ^1 Ori C, the measured [C II] line intensity corresponds to $T_P \sim 165$ K (assuming a 5 km s^{-1} line width) which is in good agreement with the value $T_P \sim 140$–150 K obtained by Boreiko et al. (1988). We have corrected their value for self-chopping (~10%–15% for their 10′ chopper throw; see Fig. 2).

3.1.2. *Orion Molecular Cloud Scan*

Figure 2 (bottom) displays the path of the [C II] cuts across the Orion molecular cloud superposed on the ^{12}CO(1–0) peak antenna temperature map of Schloerb & Loren (1982). Figure 2 (top) represents the reconstructed [C II] cuts across the Orion molecular cloud. The cuts were reconstructed by assuming that the end points contained no measurable [C II] line emission and integrating inward from both end points. For each cut, the three detectors agree rather well. Cut 1 passed very close to the BN-KL source (~18″ north-east) on the 80% contour (4.0×10^{-3} ergs s^{-1} cm^{-2} sr^{-1}) of the interface map. The observed peak intensity of the cut (4.1×10^{-3} ergs s^{-1} cm^{-2} sr^{-1}) is therefore in good agreement with the (self-chopping corrected) interface region map.

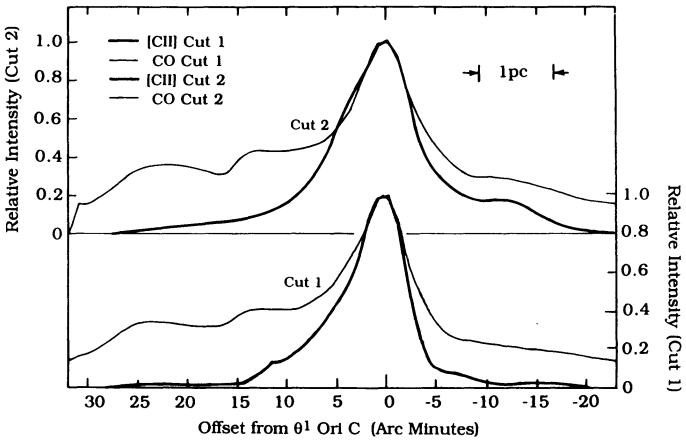

FIG. 3.—[C II] strip maps superposed on cuts through the ^{12}CO(1–0) map of Schloerb & Loren (1982). The data from the interface map have been folded in with the strip maps, and the result convolved to the resolution of the ^{12}CO (1–0) beam (2.'3).

The [C II] line emission is detectable over the entire Orion molecular cloud traced by its ^{12}CO (1–0) line emission (Fig. 3). The line is bright, at an intensity level greater than 20% of the peak for regions as far as 10′ east of Θ^1 Ori C. In addition there is a "plateau" of emission across the face of the Orion GMC, prominent in both cuts, extending $\sim$30′ to the east and $\sim$20′ to the west of Θ^1 Ori C. The plateau is particularly strong in the westernmost regions of cut 2, where the [C II] cut follows a ridge in the ^{12}CO(1–0) emission. The intensity of the [C II] emission over the face of the Orion molecular cloud is typically $\sim 1.3 \times 10^{-4}$ ergs s^{-1} cm^{-2} sr^{-1}. Such extensions of [C II] line emission were originally reported as the [C II] "halos" of M17 (Russell et al. 1981) and NGC 2024 (Kurtz et al. 1983), and more recently mapped with smaller beams for the M17 SW molecular cloud (Stutzki et al. 1988; Matsuhara et al. 1989) and the W43 complex (Shibai et al. 1991). If we assume that [C II] emission at this level extends over the entire OMC-1 complex, ($\sim 1° \times 5°$; Maddalena et al. 1986), then the integrated [C II] luminosity is $\sim$1500 $L_\odot$. Harper (1974) estimates that the FIR luminosity of the inner $\sim$10′ of the Orion molecular cloud is $\sim 3 \times 10^5$ $L_\odot$. From the *IRAS* 100 and 60 μm north-south cuts of Bally, Langer, & Liu (1991) we estimate the outer regions of the molecular cloud contribute an additional 2×10^5 $L_\odot$, so that our estimated [C II] luminosity is $\sim$0.3% of the total FIR luminosity of the Orion molecular cloud.

The degree of contaminating [C II] emission present in the endpoints of our [C II] cuts may be estimated as follows. Most of the observed [C II] emission is associated with the photodissociated surface of the molecular cloud. Over the face of the molecular cloud, from regions well removed from the interface region, the [C II]/^{12}CO(1–0) line intensity ratio is nearly constant at $\sim$1200 (see below). At the endpoints of our [C II] scan, the ^{12}CO(1–0) line intensity is $\sim$15–20 K km s^{-1} (Schloerb & Loren 1982). Therefore, the [C II] intensity at the endpoints is likely ~ 3–4×10^{-5} ergs s^{-1} cm^{-2} sr^{-1}, or about 20%–30% of the extended plateau [C II] emission from the molecular cloud.

3.2. *Far-Infrared and Submillimeter* CO *Line Emission*

We detected strong FIR and submillimeter CO line emission from both Θ^1 Ori C and the bar (Table 1). Θ^1 Ori C is $\sim$2.5 FIR beamwidths from the BN-KL outflow region, which has an intrinsic source size $\sim$40″ in the FIR CO lines (Watson et al. 1985). Therefore $\sim$2% of the FIR CO line flux from BN-KL will be in the wings of our FIR beams at Θ^1 Ori C (Harris 1988). We subtracted this contaminating flux from the observed line intensities. The bar region is sufficiently distant from the BN-KL outflow to preclude spectral contamination there. The FIR lines are unresolved at our spectral resolution, indicating an intrinsic line width of $\Delta v \lesssim 10$ km s^{-1}. This is consistent with the narrow line emission ($\Delta v_{\rm FWHM} \lesssim 5$ km s^{-1}) reported in the 17–16 transition toward Θ^1 Ori C (Boreiko, Betz, & Zmuidzinas 1989).[7] The (fully resolved) CO(7–6) lines are also narrow ($\Delta v_{\rm FWHM} \sim 7$ and 5 km s^{-1} at Θ^1 Ori C and the "bar," respectively) and are very bright with main beam Rayleigh-Jeans brightness temperatures $T_{\rm RJ} \sim 80$ and 60 K, respectively, at the Θ^1 Ori C and the "bar" (Fig. 4). With the 3′ chop amplitude used for the 7–6 observations, we estimate spectral contamination through emission in the reference beam to be $\sim$33% (Howe et al. 1992), so that the true brightness temperatures are $\sim$120 and 90 K, respectively. The Planck-corrected brightness temperatures are $T_{\rm P} \sim 140$ K, which represent the minimum gas kinetic temperatures appropriate if the emitting transition is optically thick and thermalized with unit beam filling factor. Assuming the FIR and submillimeter line emission have similar velocity distributions, the measured FIR line intensities correspond to Planck-corrected main beam brightness temperatures of $\sim$40–60 K.

[7] The integrated 17–16 line intensity that we measure toward Θ_1C is $\sim$3 times larger than the value reported by Boreiko et al. (1989). However, our observed line and continuum intensities toward BN-KL are also larger by the same factor. We use our values since our BN-KL measurements agree very well with previous independent measurements reported in the literature (Erickson et al. 1981; Stacey et al. 1982; Jaffe et al. 1984; Genzel, Poglitsch, & Stacey 1988).

TABLE 1

CO OBSERVATIONS

Position	Transition	$T_{\rm RJ}$	ΔV(FWHM) (km s^{-1})	Beam	Intensity (ergs s^{-1} cm^{-2} sr^{-1})
Θ^1 Ori C	7–6	120	7	26″	4.5×10^{-4}
	14–13	27	7	60″	8.0×10^{-4}
	17–16	15	7	54″	1.0×10^{-3}
Optical bar	7–6	90	5	26″	2.0×10^{-4}
	14–13	14	5	60″	3.1×10^{-4}

NOTE.—The CO(7–6) observations have been corrected for "self-chopping" (see text).

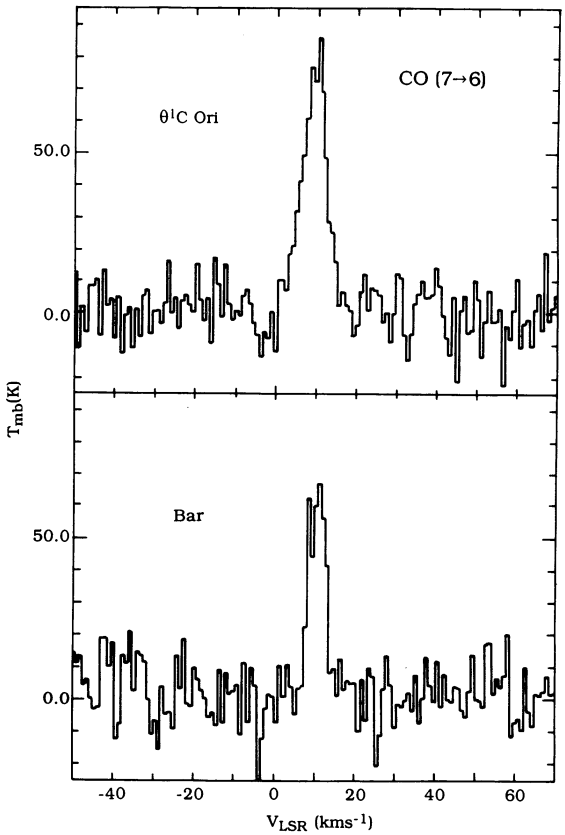

FIG. 4.—CO (7–6) spectra obtained at Θ^1 Ori C (*top*) and the optical "bar" (*bottom*).

4. DISCUSSION

4.1. *Interface Region*

4.1.1. *Physical Cordinations of the Photodissociated Atomic Gas*

H. B. Ellis, Jr., and M. W. Werner (1985, private communication) measured the intensity distribution of the bright 63 and 145 μm [O I] lines along a cut through the Trapezium cluster and BN-KL regions of Orion. We have superposed their cuts on a similar cut through our [C II] interface map in Figure 5. There is a very good correspondence between the three lines over the cut with clear evidence for enhanced [O I] 63 μm emission near the BN-KL outflow. The [O I] profile toward BN-KL consists of both narrow ($\Delta v \sim 7$ km s^{-1}) and broad ($\Delta v \sim 30$–50 km s^{-1}) velocity components, where the broad component is mostly shock-excited [O I] emission from the outflow (Werner et al. 1984; Crawford et al. 1986). Toward H_2 peak 1 (Beckwith et al. 1978) this broad line emission is $\sim$50% of the total 63 μm line flux (Crawford et al. 1986). There is no evidence for this broad component in the [C II] profiles (Boreiko et al. 1988): very little C^+ is produced in shocks (Hollenbach & McKee 1989). There is also no apparent enhancement of the 145 μm line at BN-KL. The 63 μm line is relatively much more enhanced in the BN-KL outflow than the 145 μm line due to (1) the high postshocked gas density ($n_{H_2} \sim 2 \times 10^6$ cm^{-3}; Watson et al. 1985) which favors emission from the 63 μm line ($n_{crit} \sim 4 \times 10^5$ cm^{-3}) relative to the 145 μm line ($n_{crit} \sim 6 \times 10^4$ cm^{-3}) and (2) the high optical depth in the 63 μm line from the interface region (see below) which suppresses emission at 63 μm from this narrow line component. Subtracting the shock-excited [O I] 63 μm line emission (dotted line in Fig. 5), the distributions of the [O I] and [C II] lines are very similar.

The good spatial correlation between the [O I] and [C II] lines gives strong support to the contention that the three lines arise in the same gas (cf. Stacey et al. 1983; Stacey 1985; Tielens & Hollenbach 1985a). The observations (Table 2) are compared with a model for the physical conditions of the emitting gas. The model is based on collisional excitation and treats the radiative transfer in an escape probability formalism. We use the O I/He and O I/H_2 cross sections for collisional excitation as given by Monteiro & Flower (1987) and Jaquet et al. (1992) and the C II/H_2 and C II/H cross sections of Flower & Launay (1977). The fractional abundances of O^0 and C^+ are O/H $\sim 5 \times 10^{-4}$ and C^+/H $\sim 3 \times 10^{-4}$. We assume the line widths are 5 km s^{-1}. The [O I] line intensity ratio ($I_{63\,\mu m}/I_{145\,\mu m} \sim 13$) constrains the gas pressure, $n_H T$, to be $\sim 10^8$ cm^{-3} K. The optically thick ($\tau_{63} \sim 3$) 63 μm [O I] intensity constrains the gas kinetic temperature; $T_{kin} \gtrsim 200$ K. The best model fits are $T_{kin} \sim 300$ K, $n_H \sim 4 \times 10^5$ cm^{-3}. The 145 μm [O I] and 158 μm [C II] lines have small optical depth ($\tau_{145} \sim 0.6$; $\tau_{[C\,II]} \sim 0.9$) and thereby constrain the C^+ and O^0 column densities: $N_{C^+} \sim 4.6 \times 10^{18}$ and $N_{O^0} \sim 7.7 \times 10^{18}$ cm^{-2}. The concomitant hydrogen column density is $N_H \sim 1.5 \times 10^{22}$ cm^{-2} ($A_V = 7.5$), or $\sim$3% of the total molecular hydrogen column density estimated for the "spike" component in the interface region ($N_{H_2} \sim 2.5 \times 10^{23}$ cm^{-2}; Wilson et al. 1986). Integrated over the interface region map, the total

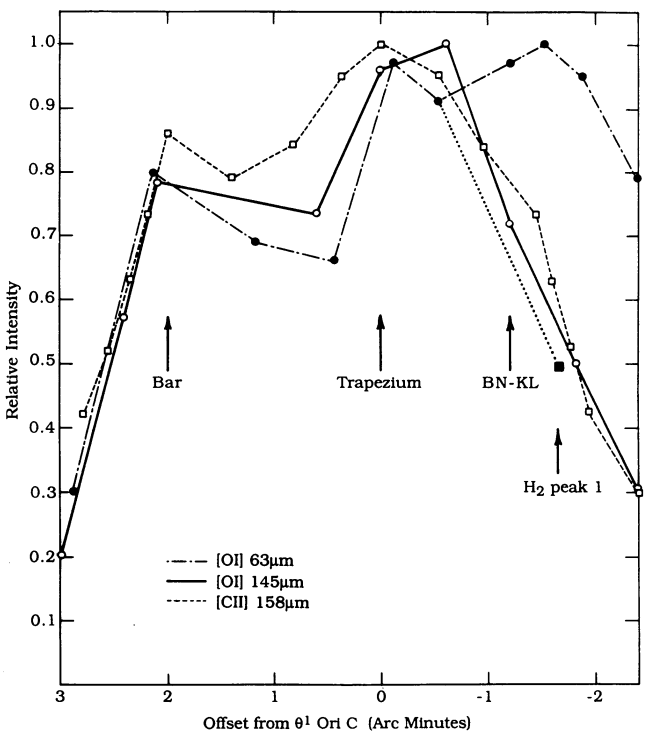

FIG. 5.—Cuts in the 63 and 145.5 μm fine-structure lines of O^0 and the 158 μm C^+ fine-structure line through the Orion H II region/GMC interface. The cut runs through Θ^1 Ori C and BN-KL (position angle $\sim$150°). The peak intensities, and beam sizes for the three data sets are given in Table 2. The [O I] data are from H B. Ellis, Jr., & M. W. Werner (1985, private communication). The [C II] cut is from this work. The filled square is an estimate of the narrow line flux in the 63 μm [O I] line at H_2 peak 1 (Crawford et al. 1986). The dotted line is the observed 63 μm [O I] cut minus the shocked emission from the BN-KL outflow region.

TABLE 2

FINE-STRUCTURE LINE OBSERVATIONS

Species	Transition	Wavelength (μm)	Beam	Intensity (ergs s^{-1} cm^{-2} sr^{-1})
O^0	$^3P_0 \rightarrow {}^3P_1$	145.525	53″	4.2×10^{-3}
	$^3P_1 \rightarrow {}^3P_2$	63.184	30″	5.4×10^{-2}
C^+	$^2P_{3/2} \rightarrow {}^2P_{1/2}$	157.741	55″	5.0×10^{-3}

NOTES.—[O I] intensities are from Werner et al. 1984 (63 μm) and H. B. Ellis, Jr., & M. W. Werner 1985, private communication (145 μm). The fluxes are taken at the peak of the [C II] interface region map.

hydrogenic mass contained in the photodissociation region is ~ 50–$100\ M_\odot$.

These results are in good agreement with the physical parameters obtained with photodissociation region models of the Orion interface region ($265 < T_{gas} < 500$ K, $n_H \sim 1$–2×10^5 cm^{-3}, $N_{C^+} \sim 3$–4×10^{18} cm^{-2}, $\tau_{[C\ II]} < 1$; Tielens & Hollenbach 1985b; Wolfire, Tielens, & Hollenbach 1990). The physical parameters of the emitting gas may also be derived from the [^{12}C II] to [^{13}C II] fine-structure line intensity ratio, assuming a $^{12}C/^{13}C$ abundance ratio. At Θ^1 Ori C, taking a $^{12}C/^{13}C$ abundance ratio of 43 (cf. Hawkins & Jura 1987; Johansson et al. 1984), Stacey et al. (1991b) obtain $T_{gas} \sim 310$ K, $N_{C^+} \sim 4.1 \times 10^{18}$ cm^{-2}, and $\tau_{[C\ II]} \sim 0.75$, in good agreement with the results obtained here. These coupled analyses therefore support values near 43 for the $^{12}C/^{13}C$ abundance ratio in the Orion molecular cloud.

4.1.2. *Warm, Quiescent CO Emission from the Interface Region*

Figure 6 (left) superposes the KAO (98″ beam) CO(7–6) peak T_A^* map of the interface regions of the Orion nebula (Schmid-Burgk et al. 1989) on the contours of ^{12}CO(1–0) brightness temperature (Schloerb & Loren 1982, 50″ beam). The CO(1–0) brightness temperature map traces the narrow "spike" feature in the CO line emission and largely suppresses the broad line contribution from the BN-KL outflow. There is excellent spatial correspondence between the maps, suggesting that the millimeter CO lines from the interface region arise from the same gas which produces the submillimeter 7–6 line. The [C II] interface map is superposed on the CO(1–0) map in Figure 6 (right). Again, there is a good correspondence between the two distributions, demonstrating that the [C II] and CO(1–0) lines arise from closely associated regions. This correspondence is particularly good for an east-west cut across the interface near Θ^1 Ori C (Fig. 7). In addition, there is a very good *spectral* correspondence between the warm molecular and photodissociated gas. Figure 8 superposes our CO(7–6) profile from Θ^1 Ori C on the [C II] profile (Boreiko et al. 1988). The spectral profiles are very similar, demonstrating similar velocity dispersions in the photodissociated atomic and warm molecular gas. The similarities in spatial extent, distribution, and spectral profile between the CO(7–6), CO(1–0) "spike" emission and the [C II] line emission suggests that the "spike" feature apparent in the CO emission arises in gas physically associated with the [C II]–emitting gas in the interface region.

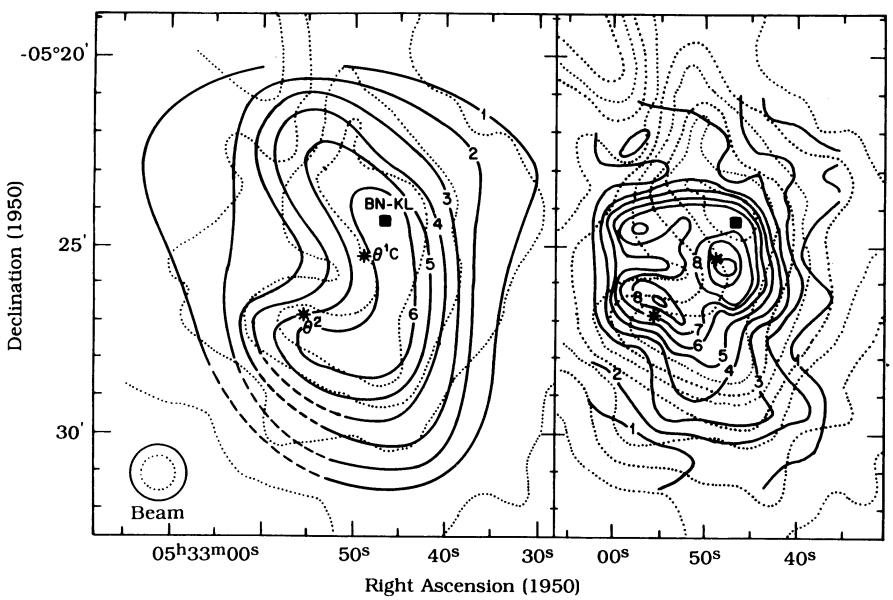

FIG. 6.—(*left*) CO(7–6) peak T_A^* map of the interface region of the Orion nebula (Schmid-Burgk et al. 1989; 98″ beam, solid lines, contour interval 10 K) superposed on contours of ^{12}CO(1–0) brightness temperature (Schloerb & Loren 1982, 50″ beam, dotted lines, contour interval 20 K, peak contour 100 K). (*right*) [C II] map of the interface region (Fig. 1, 55″ beam, solid lines) superposed on the CO(1–0) peak brightness temperature map (Schloerb & Loren 1982, dotted lines, contour interval 10 K, peak contour 110 K).

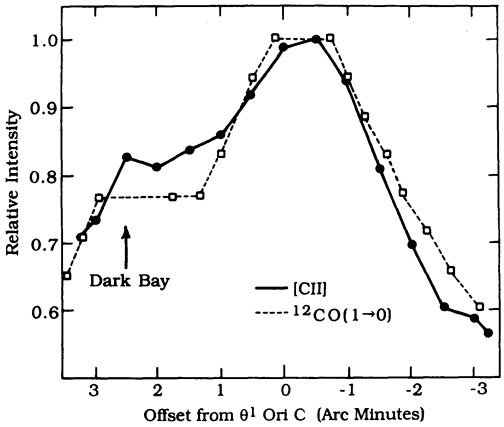

FIG. 7.—East-west slice through the [C II] and CO(1–0) maps of Fig. 6 taken at the declination of Θ^1 Ori C. This east-west cut avoids shock-excited CO emission associated with the BN-KL outflow.

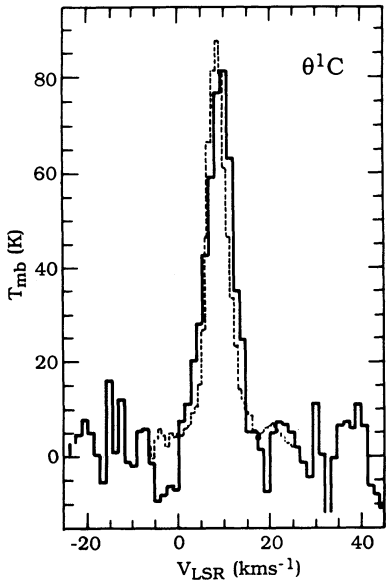

FIG. 8.—[C II] spectrum (Boreiko et al. 1988; 45″ beam) superposed on our CO(7–6) spectrum (26″ beam). Both spectra were taken at Θ^1 Ori C.

4.1.3. *Physical Conditions of the Molecular Gas*

The CO-emitting gas in the interface region must be both warm ($T_g \gtrsim 140$ K) and dense ($n_{H_2} \sim 1.4 \times 10^4$ cm^{-3}) to account for the observed brightness of the FIR CO lines. We have calculated the CO level populations for the lowest 30 rotational levels in an escape probability, radiative transfer formalism. We use collision cross sections from Schinke et al. (1985) and Flower & Launay (1985). Figure 9 plots our observed line intensities along with the Lower J ^{12}CO and ^{13}CO line intensities available in the literature as a function of J_{upper}. The ^{12}CO and ^{13}CO line intensities are used together with an assumed ^{12}CO/^{13}CO abundance ratio to solve for the physical parameters of the emitting gas. These parameters are largely driven by the need to substantially populate the upper rotational levels to account for the large observed FIR and submillimeter rotational line intensities. The observed intensity of the ^{13}CO(6–5) line requires that the column density of ^{13}CO be in excess of 4×10^{16} cm^{-2} (Graf et al. 1990). For these column densities, the large ^{12}CO(14–13)/(7–6) line intensity ratio ($\sim$1.5–2) requires pressures in excess of 1×10^6 K cm^{-3}. The emitting gas must have temperatures in excess of 100 K to account for the observed brightness of the ^{12}CO(7–6) and 6–5 lines, and densities $\lesssim 5 \times 10^4$ cm^{-3}, to be consistent with the relative weakness of the ^{12}CO(17–16) and 14–13 lines. With

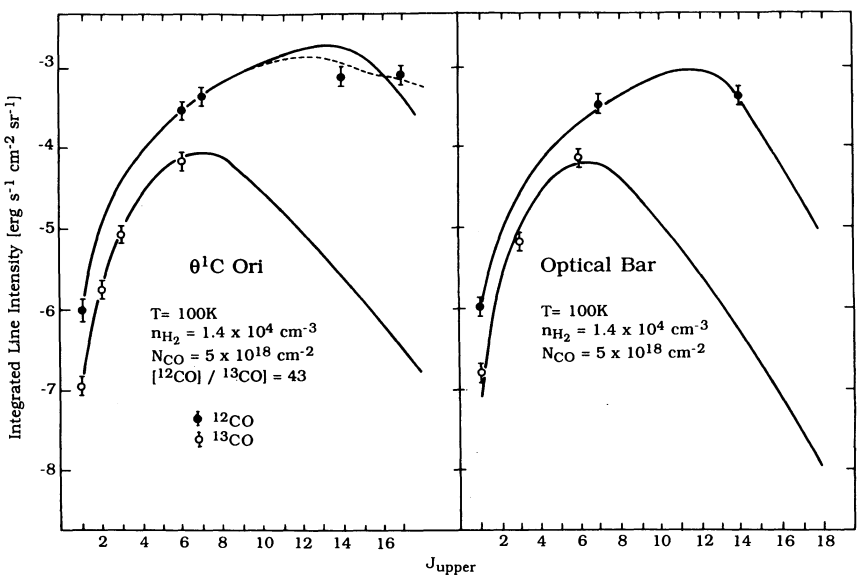

FIG. 9.—Observed CO line intensities as a function of the upper state rotational quantum number, J_{upper}, for regions near Θ^1 Ori C and the "bar" (see Table 1). The solid lines represent our "best-fit" single component modeling of the observed intensities as a function of J_{upper}. The dashed line represents the two component model for the emission from Θ^1 C Ori (component 1: $n_{H_2} = 4 \times 10^3$ cm^{-3}, $T_{kin} = 140$ K, $N_{CO} = 7 \times 10^{18}$ cm^{-2}; component 2: $n_{H_2} = 3 \times 10^5$ cm^{-3}, $T_{kin} = 500$ K, $N_{CO} = 8 \times 10^{16}$ cm^{-2}). The CO transition, beam size, and reference are ^{12}CO(1–0), 50″, Schloerb & Loren 1982; ^{12}CO(6–5), 35″, Koepf et al. (1982); ^{12}CO(7–6), (14–13), (17–16), this work (Table 1); ^{13}CO(1–0), 55″, Schloerb & Loren 1982; ^{13}CO(2–1), 33″, Howe et al. (1992); ^{13}CO(3–2), 15″, Graf et al. (1990); ^{13}CO(6–5), 8″, Graf et al. (1990).

these constraints, and assuming a $^{12}CO/^{13}CO$ abundance ratio of 43, the best-fit single-component model for Θ^1 Ori C is, $n_{H_2} \sim 1.4 \times 10^4$ cm^{-3} and $T_{kin} \sim 140$ K, $N_{CO} \sim 7 \times 10^{18}$ cm^{-2}. For the "bar" region, $n_{H_2} \sim 1.4 \times 10^4$ cm^{-3}; $T_{kin} \sim 100$ K, $N_{CO} \sim 5 \times 10^{18}$ cm^{-2}. If the $^{12}CO/^{13}CO$ abundance ratio were 67 (cf. Langer & Penzias 1990), the best-fit models would have the same gas temperature, but require ^{12}CO column densities that are 1.6 times larger, and gas densities that are 1.4 times smaller ($\sim 10^4$ cm^{-3}) than the lower abundance ratio fits. The smaller densities substantially lower the populations in the FIR rotational levels to compensate for the larger ^{12}CO column densities which would otherwise result in too strong emission in the optically thin FIR lines. The gas kinetic temperature and column densities for these models are similar to those given by Graf et al. (1990) based on models of the ^{13}CO(6–5) and 3–2 lines. The gas density, however, is poorly constrained by the mid-J emission reported by Graf et al. (1990). Our observations of the ^{12}CO FIR rotational lines provide this density constraint.

The model fits are fairly good for most of the ^{12}CO and ^{13}CO lines except for the FIR (J = 14–13 and 17–16) lines at Θ^1 Ori C (solid lines, Fig. 9). Since these are the highest excitation lines, they are the most sensitive to the model parameters. Clearly our single-component model is unrealistic, and it is likely that a multiple-component model comprising a range of temperatures and densities will yield a better fit to the FIR data. For example, a two-component model, which separates the emission in the lower J lines from the FIR lines, gives a significantly better fit to the data. Parmar, Lacy, & Achtermann (1991) detected H_2 rotational line emission from the "bar" which indicates the presence of a very warm ($T_{kin} \sim 500$ K), modest column density ($N_{H_2} \sim 10^{21}$ cm^{-2}) component to the molecular gas. If the density of this gas is fairly high ($n_{H_2} \sim 3 \times 10^5$ cm^{-3}), this component alone fits both the absolute and relative intensities of the 17–16 and 14–13 lines observed at Θ^2 Ori C. The high gas pressures in such a model result in small populations in the lower J levels, so that this component does not significantly affect the lower J emission. The lower J emission is therefore roughly modeled as a separate component superposed on this high-pressure solution. The best-fit model for the lower J lines is similar to the best-fit single-component model described above, except that the gas density is substantially lower ($n_{H_2} \sim 4 \times 10^3$ cm^{-3}) to limit the emission in the FIR lines. This two-component model is plotted as a dashed line in Figure 9 (left).

For our models, the mid-J ^{12}CO lines are optically thick and thermalized. Since the main beam brightness temperature of the transition is about the same as the gas temperature, the beam area filling factor for the emitting gas must be near unity. Assuming an abundance ratio $[CO]/[H_2] = 8 \times 10^{-5}$ the hydrogen column density in the warm emitting gas is $N_{H_2} \sim 9 \times 10^{22}$ cm^{-2}, or about 35% of the total molecular hydrogen column density estimated for the Orion molecular cloud ($N_{H_2} \sim 2.5 \times 10^{23}$ cm^{-2}; Wilson et al. 1986). The total mass of the warm molecular component, integrated over the interface region, is $\sim 500\ M_\odot$.

4.1.4. *Excitation Mechanisms for the Warm Molecular Gas*

Bright, narrow line width CO submillimeter and FIR line emission has previously been reported from the M17 interface region and S106 (Harris et al. 1987b), NGC 2023 (Jaffe et al. 1990), and the Orion interface region (Schmid-Burk et al. 1989; Graf et al. 1990). Shock excitation of this warm, quiescent CO is almost certainly ruled out on the basis of the observed narrow line profiles ($\Delta v_{FWHM} \lesssim 5$ km s^{-1}). Furthermore, Graf et al. (1990) estimate that ~ 700 shock fronts are required along the line of sight toward the Orion interface to account for the observed brightness of the ^{13}CO(6–5) line. Gas-dust collisions are also ruled out for the Orion interface region. The dust temperatures required just to account for the observed short submillimeter line emission (~ 115 K; Graf et al. 1990) are greatly in excess of those observed (~ 50 K; Werner et al. 1976). In addition, the gas density derived above is too small to permit efficient gas-grain thermal coupling. The requirements for the FIR line emission reported here are even more severe.

Due to the observed correlation between short submillimeter CO line intensity and FUV field strength, the most likely source of the energy to heat the molecular gas is the local FUV radiation field (Graf et al. 1990). However, while current photodissociation region models (Tielens & Hollenbach 1985a; Sternberg & Dalgarno 1989; Burton, Hollenbach, & Tielens 1990) may account for the submillimeter line emission observed from molecular clouds exposed to low levels of FUV radiation (Jaffe et al. 1990), the models fail by more than an order of magnitude to reproduce the large column densities of warm CO gas required to explain the observed ^{13}CO(6–5) line emission from the Orion interface region (Graf et al. 1990). In spite of this theoretical problem, the association of atomic and molecular gas makes an explanation involving FUV heating particularly attractive.

4.2. *Orion Molecular Cloud*

4.2.1. *Origin of the Extended* [C II] *Emission*

Carbon-ionizing FUV photons penetrate molecular clouds to $\tau_{UV} \sim$ a few, or $A_V \lesssim 5$, limited primarily by the absorption of these photons by dust (Werner 1970). We therefore expect that the column density hydrogenic nuclei in the C^+ zone associated with the Orion interface region to be $\lesssim 10^{22}$ cm^{-2} in reasonable agreement with the modeling for the interface region given above. Using the derived density for the emitting region, $\sim 4 \times 10^5$ cm^{-3}, the penetration of the carbon ionizing photons for a simple uniform model is $\sim 3 \times 10^{16}$ cm^{-2} or $\lesssim 4''$ at the distance of Orion. On this basis, one would expect that the observed [C II] emission would drop off within one beam outside the bowl-shaped H II region. In fact, the [C II] line emission does drop off rather sharply, but the drop-off is *resolved* with a scale length of the order 5′. Even more surprising is the extended "plateau" of [C II] emission which is apparent in the east-west cuts across the Orion molecular cloud. What is the origin of this extended emission?

The most natural explanation for both the large scale length of the observed drop-off in [C II] emission from the interface region *and* the extended [C II] emission from the Orion molecular cloud itself is in terms of the geometry of the Orion H II region/GMC interface region. The extended [C II] component may simply be the result of FUV photons from the Trapezium cluster escaping the H II region from the density-bounded side of the Orion H II region and impinging on the Orion molecular cloud. The observed extended carbon radio recombination line emission from Orion may also arise from the surface layers of the molecular cloud consistent with this model (Jaffe & Pankonin 1978). In the simplest model we assume that there is no intervening material along the line of sight between the Trapezium cluster and the "greater molecular cloud." If r[pc] denotes the observed (projected) distance between the Trape-

zium cluster and a point along our E-W cut through the Orion molecular cloud, then the FUV field strength at r is given by

$$\chi_{\rm geometric}(r) = C \times r_b/(r^2 + r_b^2)^{3/2} ,$$

where r_b is the distance (along our line of sight to Orion) between the Trapezium cluster and the Orion GMC, C is a constant, and the ambient FUV (6.2 eV $< h\nu <$ 13.6 eV) ISRF, $\chi(r)$, is normalized in units of the local ISRF ($\chi_0 = 1 \equiv 2.0 \times 10^{-4}$ ergs s^{-1} cm^{-2} sr^{-1}; Draine 1978). The FUV field intensity at the Orion H II region/GMC interface ($r = r_0 \equiv$ 0.39 pc (2.'8) is $\chi(r_0) \sim 5.1 \times 10^4$ (Stacey et al. 1991a), so that assuming $r_b \sim r_0$, $C \sim 2.2 \times 10^4$. The model is insensitive to the value taken for r_b. For the discussion which follows, we use the predictions of the photodissociation region models presented in Sternberg & Dalgarno (1989) and Stacey et al. (1991a). These models are similar to those of Tielens & Hollenbach (1985a) and van Dishoeck & Black (1988).

Assuming the cloud density, one may predict the expected [C II] intensity from the Orion molecular cloud at a given radius from the H II region. For the "plateau" regions of [C II] emission, ($r \sim 2.5$ pc; $\chi_{\rm geometric} \sim 500$) we would expect a [C II] intensity of $\sim 10^{-3}$ ergs s^{-1} cm^{-2} sr^{-1} if the densities are between 10^3 and 10^5 cm^{-3}. The observed intensity is 8 times smaller than this—the geometrically diluted FUV field strength is 20 times larger than that required to produce the observed [C II] intensity ($\chi_{\rm UV} \sim 25\chi_0$; see below). The challenge with this model, therefore, is not how to explain the extended emission, but rather how to keep it so small. This is naturally accomplished by allowing absorbing gas to intervene along the line of sight between the Trapezium cluster and the molecular cloud. The observed [C II] line intensity is then used along with the PDR model to predict the required UV field strengths assuming unit beam filling factor and reasonable cloud densities: $n_{\rm H_2} \sim$ few $\times 10^3$ cm^{-3} (outer cloud) to $\sim$few $\times 10^5$ cm^{-3} (interface region).

Figure 10 represents the results of such modeling. For the top panel, the solid and dashed lines are the observed [C II] line intensity as a function of projected distance from Θ^1 Ori C for the two cuts across the molecular cloud. For regions within 3′ of Θ^1 Ori C, we use the fully sampled interface map to fill in the details of the molecular cloud scans. The bottom panel displays the FUV flux available from the geometric dilution of the flux from the Trapezium cluster ($\chi_{\rm geometric}[r]$; dotted and dot-dashed lines) and the FUV fluxes required to produced the observed [C II] emission ($\chi_{\rm theoretical}[r]$; solid and dashed lines) for the two cuts. Here $\chi_{\rm theoretical}(r)$ is the FUV flux theoretically required to yield the observed [C II] intensity at r. Also plotted on the top panel (dotted and dot-dashed lines) are the FUV extinctions required to attenuate the geometrically diluted FUV flux from the Trapezium cluster such that the incident fields are consistent with the observed [C II] intensity: $A_{\rm UV}(r) = -2.5$ log ($\chi_{\rm theoretical}[r]/\chi_{\rm geometric}[r]$). Flat regions of the right ascension offset–$A_{\rm UV}$ plane are regions where there is little intervening dust. Steeply sloped regions indicate large amounts of absorbing material.

For the interface region of the nebula ($r <$ 2.'5) the model indicates there is essentially no extinction—the full FUV flux from the Trapezium cluster is required to yield the observed [C II] intensity. Beyond 2.'5, however, the [C II] intensity falls rapidly, indicating large amounts of absorbing dust. The two cuts are spatially coincident for the regions to the east of the Trapezium cluster, so the extinction derived as a function of

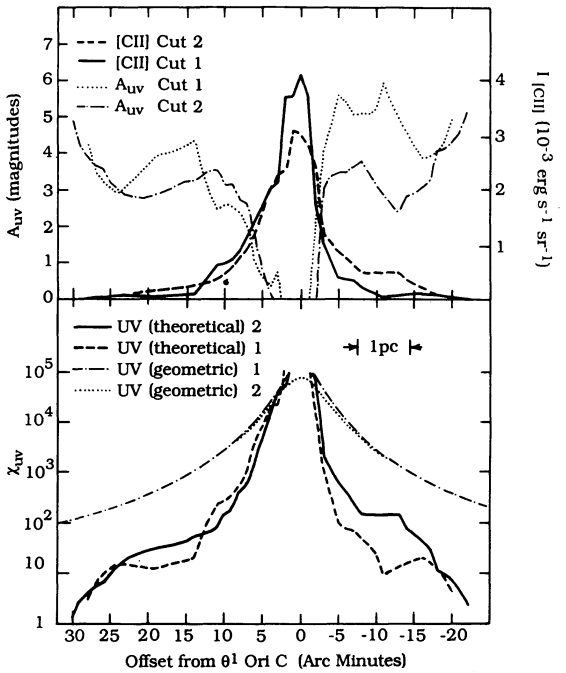

FIG. 10.—(*top*) [C II] intensities (*solid and dashed lines*) as a function of R.A. offset from Θ^1 Ori C for the two cuts across the Orion molecular cloud. FUV extinction (*dotted and dot-dashed lines*) between the Trapezium cluster and the molecular cloud as a function of distance from the cluster. (*bottom*) Geometrically diluted FUV field from the Trapezium cluster (*dotted and dot-dashed lines*) and the FUV field theoretically required by the brightness of the [C II] emission (*solid and dashed lines*) for the two cuts across the Orion GMC. Data from the interface map have been folded into the cuts across the molecular cloud. The theoretical curves (and consequently, the FUV extinction curves) do not close in the interface regions, as the single layer standard PDR model predicts a smaller [C II] intensity from the interface region than the observed value (Tielens & Hollenbach 1985b). The observed [C II] intensity may be enhanced by geometric effects (multiple PDR layers or tilting of a single layer), or through a smaller ratio for the FUV to visual extinction ($A_{\rm UV} \sim A_V$) than is present in the diffuse interstellar medium (Tielens & Hollenbach 1985b).

offset east of the Trapezium is the same for both cuts. The region of extinction to the east begins 3′ east of Θ^1 Ori C, and the extinction grows linearly to 9′ east. Farther east, there is apparently very little additional extinction. The intervening gas presents $\sim$3.0 magnitudes of extinction in the FUV, or $A_V \sim 1.7$ ($A_{\rm UV} = 1.8\ A_V$). The corresponding column density of hydrogen is $\sim 3.4 \times 10^{21}$ cm^{-2} ($A_V = 1 \Leftrightarrow N_{\rm H} = 2 \times 10^{21}$ cm^{-2}). The angular extent of the region ($\sim$6′) corresponds to 0.84 pc at the distance of Orion, so the mean density of the region is $\sim 1.3 \times 10^3$ cm^{-3}. To the west of the H II region, the [C II] emission falls off rapidly outside a 2′ radius. Cut 1 runs nearly east-west and indicates absorbing gas between 2′ and 7′ ($A_{\rm UV} \sim 5$) from the H II region. Cut 2, which runs at an angle of 4.°7 north of east, indicates a gas cloud between 3′ and 4.'3 ($A_{\rm UV} \sim 3.0$). The corresponding mean densities of these clouds are $\sim 2.5 \times 10^3$ cm^{-3} and 6×10^3 cm^{-3}, respectively. At both ends of both cuts our model indicates a rapid rise in the inferred FUV extinction, that is, there is less observed [C II] radiation than would be predicted through the geometric dilution of the FUV flux from the Trapezium cluster. This drop-off in [C II] emission simply represents the edges of the Orion molecular cloud. Figure 11 illustrates the geometry involved with our model.

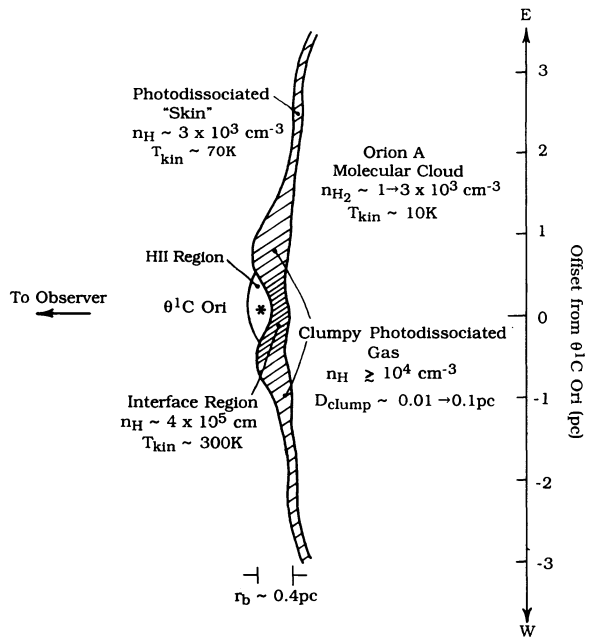

FIG. 11.—Proposed geometry of the Orion H II region/GMC interface. North is out of the page, and the observer at Earth is to the left.

4.2.2. *The Orion PDR is Clumpy*

Bright CO(7–6) line emission is observed from the absorbing gas regions, indicating that the minimum gas density in these regions is $\sim 10^4$ cm^{-3} (Howe et al. 1992). The [C II] and [O I] line intensity ratios are roughly constant across the interface region (Fig. 5) so the gas density in the absorbing gas regions may be as large as that of the interface: 4×10^5 cm^{-3}. Since the average gas density is $\sim$few $\times 10^3$ cm^{-3}, the obscuring material must be clumpy with volume filling factors, Φ_V, between $\sim$1% and 50%. Assuming spherical or thin sheet geometry for these clumps, the characteristic clump size is given roughly by $D_{cloud} \times \Phi_V/\Phi_A$, where D_{cloud} is the source size and Φ_A is the beam area filling factor. The value of ϕ_A is near unity for the [C II] emission, so with the observed sources sizes above, we obtain a characteristic clump scale size $D_{clump} \sim 4''$–$50''$ (0.01–0.12 pc). This characteristic size is similar to that obtained through high spatial resolution CS(2–1) mapping of the Orion interface region ($\sim 10''$; Mundy et al. 1986). Analyses based on [C II] mapping of other Galactic molecular clouds require similar clumping factors and clump sizes (e.g., Sgr A, Genzel et al. 1985; M17 SW, Stutzki et al. 1988; and W3 and NGC 1977; Howe et al. 1991).

Howe et al. (1992) also concluded that the Orion molecular cloud was clumpy based on CO(7–6) and ^{13}CO(2–1) right ascension cuts through the Trapezium. Their cuts extend from $\sim 9'$ east to $\sim 5'$ west of Θ^1 Ori C. In the regions between $\sim 3'$ and $9'$ east of the Trapezium cluster the line profiles are split into at least two velocity components. High spectral resolution measurements of the C109α carbon recombination line (Jaffe & Pankonin 1978) and the [C II] line at $4'$ east of Θ^1 Ori C (Boreiko et al. 1988) indicate that these lines are similarly split. The persistence of these velocity components over arcminute length scales makes it unlikely that the lines are emitted at the surface of the molecular cloud, but rather signals the presence of two or more clumps along the line of sight. Howe et al. argue that the energy source for heating of the molecular gas traced through its CO(7–6) emission is likely to be the FUV flux from the Trapezium cluster. The persistence of the CO(7–6) emission over parsec scales into the molecular cloud then requires that the cloud be clumpy to allow penetration of the FUV photons.

In summary, the observed [C II] line emission observed across the face of the Orion molecular cloud probably arises from PDRs formed as a thin skin on the GMC surface by UV flux which has escaped the Orion H II region. The ultimate energy source for this extended [C II] radiation is therefore the Trapezium OB star cluster. The molecular cloud which half envelopes the H II region "blister" is clumpy, with clump densities $\gtrsim 10^4$ cm^{-3} and a clump-interclump contrast in excess of 5 to 10. The FUV light from the Orion H II region penetrates this clumpy gas giving rise to the observed extended [C II] emission. The intervening material apparently largely ends beyond regions more than $\sim 10'$ east (or $6'$ west) of Θ^1 Ori C, allowing the residual FUV flux to fall upon the extended molecular cloud.

4.2.3. *Physical Conditions of the Orion GMC Surface*

The observed [C II] intensity from the extended regions of the Orion GMC ($\sim 1.3 \times 10^{-4}$ ergs s^{-1} cm^{-2} sr^{-1}) is well fitted by PDR models with $\chi_{UV} \sim 25\chi_0$, $n_H \sim 3 \times 10^3$–10^4 cm^{-3} (Fig. 10). For these FUV field strengths and gas densities, the gas kinetic temperature is ~ 70 K (Wolfire, Tielens, & Hollenbach 1990). The requisite C^+ column density is therefore 2.5–4×10^{17} cm^{-2} ($n_H = 10^4$–3×10^3 cm^{-3}; Stacey 1985), which corresponds to $N_H \sim 7$–12×10^{20} cm^{-2} (assuming $C^+/H = 3 \times 10^{-4}$). The molecular densities near the observed regions are $n_H \sim 3 \times 10^3$ cm^{-3}, so that $\Phi_V \sim 1$ for the low-density solution. For the higher density (10^4 cm^{-3}) solution, the filling factor is ~ 0.3, so that the "depth" of the photodissociated "skin" is roughly the same in either case: $D_{PDR} \sim 3 \times 10^{17}$ cm (0.10 pc). If this "skin" extends over the entire Orion GMC, the total photodissociated mass is $\sim 3 \times 10^3$ $M_\odot$, or $\sim 3\%$ of the mass of the Orion molecular cloud (10^5 $M_\odot$; Maddalena et al. 1986).

4.2.4. *Other Sources for the Extended FUV Fields?*

Stutzki et al. 1988 (see also Matushara et al. 1989) observed extended [C II] emission across the M17 SW molecular cloud. Due to the edge-on geometry of the M17 interface region, they argue that the observed "plateau" emission is not generated by FUV flux from the OB star cluster, but rather must arise from elevated ambient FUV fields, or from FUV sources (B stars) embedded in the molecular cloud. Such mechanisms, of course, may also be present for Orion. For example, if the observed plateau emission from Orion is powered by the ambient FUV radiation field (not spillover from the Trapezium), that field must be ~ 25 times the local interstellar radiation field. Alternatively, embedded B stars may provide the requisite FUV flux. Stutzki et al. (1988) estimate that ~ 100 B stars (total luminosity $\sim 1 \times 10^5$ $L_\odot$) will form in a 10^5 $M_\odot$ molecular cloud during the cloud's lifetime. Assuming that half of these stars have already formed, and that $\sim 35\%$ of the B star luminosity comes out in the FUV (6.2 eV $< h\nu <$ 13.6 eV) band, the average FUV field within the cloud would be $\sim 3\chi_0$. This is about 10 times too small to explain the observed extended [C II] emission. However, clumping effects may increase the efficiency of conversion of the FUV intensity to [C II] intensity by an order of magnitude (Howe et al. 1991). Therefore, embedded B stars may well provide much of the required FUV flux—if the interior of the Orion molecular cloud is clumpy. However, the apparent smoothness of the

extended [C II] distribution and the geometric falloff in the required FUV fields in the outer regions of the cloud (Fig. 10) favor the simpler spillover model described above.

4.2.5. *Consequences for the Extended* [C I] *Radiation*

Phillips & Huggins (1981) have detected 610 μm [C I] line emission over an east-west scan over the entire Orion molecular cloud traced by its ^{12}CO(1–0) emission. [C I] line emission is expected to occur in photodissociation regions; however, the large apparent FUV extinction from Θ^1 Ori C to the extended [C I] emission ($\gtrsim$10 mag for the regions 30′ east assuming $n_{H_2} \gtrsim 3 \times 10^3$ cm^{-3}; Maddalena et al. 1986) appears to rule out such an origin for the extended emission. A variety of physical mechanisms were proposed to explain this extended [C I] emission including (cf. Keene et al. 1985) (1) time-dependent chemistry of the molecular cloud (cf. Langer 1976), which demonstrates that the conversion of atomic carbon to CO takes greater than 10^6 yr, leaving excess C^0 abundance in younger clouds; (2) for evolved clouds, turbulence and shocks may return some of the carbon to atomic form (cf. Boland & de Jong 1982); (3) cosmic-ray-induced, electronic excitation of H_2 may create a weak FUV field which maintains some of the carbon in atomic form (cf. Prasad & Tarafdar 1983); or (4) if the carbon-to-oxygen ratio in the parent cloud is greater than unity, excess carbon remains in the form C^0 (Langer et al. 1984).

While some of these mechanisms for producing extended [C I] emission may be still viable, the observed extended [C II] emission provides a clue to a more natural explanation. Figure 12 overlays our observed [C II] cuts on the measured [C I] distribution of Phillips & Huggins (1981). The observed [C II] emission is at least as extensive as that of [C I]. However, in contrast to C^0, the chemical models cannot produce detectable amounts C^+ (e.g., Gredel, Lepp, & Dalgarno 1987). Furthermore, the FUV fields produced in shocks or those induced by cosmic rays are far too weak to account for the intensity of the extended [C II] emission. The only known mechanism for producing [C II] radiation at the observed intensity levels is through the ionizing starlight of nearby OB stars or the general interstellar radiation field. We have argued above that the extended [C II] emission is best explained by "leakage" of the FUV radiation from the Trapezium cluster through absorbing gas clouds and onto the Orion molecular cloud forming extended photodissociation regions. We expect enhanced [C I] emission from these regions as well.

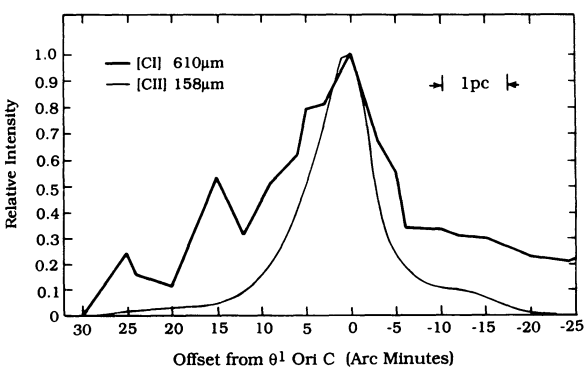

FIG. 12.—Cuts in right ascension of [C I] 610 μm emission (*darker line*; Phillips & Huggins 1981) superposed on our [C II] cuts (*lighter line*). We have averaged our two [C II] cuts and convolved the result to match the spatial resolution of the [C I] cut (2′.5).

4.2.6. ^{12}CO(*1–0*) *and* [C II] *Line Emission: the Extragalactic Connection*

Our [C II] cuts across the Orion molecular cloud provide an important link between photodissociation regions in the Galaxy and those in other galaxies. In particular, our measurements indicate that the molecular medium in normal nonstarburst galaxies may be constructed through a superposition of Galactic-type giant molecular clouds. However, the molecular medium in starburst nuclei may not be constructed from such a superposition (Stacey et al. 1991a). Therefore, this GMC–spiral galaxy link forms the basis for the contention that the molecular medium in starburst nuclei is different than that of normal spiral galaxies (Crawford et al. 1985; Stacey et al. 1991a).

The [C II] cuts across the Orion molecular cloud demonstrate that [C II] emission is correlated with that of ^{2}CO(1–0) on parsec scales, hence confirming the notion that [C II] emission is linked with molecular clouds. The [C II] line intensity for the outer regions of the Orion molecular cloud is $\sim 1.3 \times 10^{-4}$ ergs s^{-1} cm^{-2} sr^{-1}. The ^{12}CO(1–0) line intensity is $\int T_R^* dV \sim 70$ K km s^{-1} (Schloerb & Loren 1982), or $\sim 1 \times 10^{-7}$ ergs s^{-1} cm^{-2} sr^{-1} in equivalent intensity units (1 K – km s^{-1} $\Leftrightarrow$ 1.6×10^{-9} ergs s^{-1} cm^{-2} sr^{-1}; cf. Stacey et al. 1991a). The line intensity ratio is therefore $\sim$1200 for the outer regions of the Orion molecular cloud. This line intensity ratio is similar to that obtained for the outer regions of the M17 molecular cloud ($\sim$1000; Matsuhara et al. 1989).

About 70% of the observed [C II] emission from the nuclei of nonstarburst spiral galaxies arises in PDRs associated with molecular clouds (Madden et al 1992; Stacey et al. 1992). The remainder probably arises from low-density H II regions and to a lesser extent from atomic clouds. The fraction is likely similar for the inner regions of the Galaxy (Stacey et al. 1985; Stacey 1985; Shibai et al. 1991). The *observed* [C II]/^{12}CO(1–0) line intensity ratio from the Galaxy ($\sim$1250) is the same as that for a sample of eight nonstarburst nuclei (Stacey et al. 1991a). The actual line intensity ratio for the emission which originates from PDRs associated with molecular clouds is therefore $\sim$900 (Table 3)—similar to that obtained for the Orion and M17 molecular clouds. In addition, both the observed [C II]/FIR continuum intensity ratio ($\sim 3 \times 10^{-3}$) and the gas mass fraction (2%–3% relative to molecular gas) contained in PDRs is the same for the nuclei of nonstarburst galaxies and the Orion molecular cloud (Table 3). The interstellar medium in the nuclei of nonstarburst galaxies is there-

TABLE 3

COMPARISON BETWEEN GALACTIC AND EXTRAGALACTIC PHOTODISSOCIATION REGIONS

Parameter	Orion Interface	Orion GMC	Starburst Nuclei	Nonstarburst Nuclei
$I_{[C\,II]}/I_{CO}$	4500	1200	4000	900
$I_{[C\,II]}/I_{FIR}$	3×10^{-4}	3×10^{-3}	3×10^{-3}	3×10^{-3}
χ_{UV}/χ_0	5×10^4	10–100	10^3	10–200
M_{PDR}/M_{H_2}	$\sim$3%	$\sim$3%	>10%	>2%

NOTES.—References are to this work and Stacey et al. 1991a. We have assumed 70% of the observed [C II] emission from the nuclei of nonstarburst galaxies arises from PDRs associated with GMCs. For starburst nuclei, this fraction is substantially higher ($\sim$90%).

fore consistent with a superposition of Orion-like molecular clouds—supporting the contention that most of the observed [C II] line radiation from galactic nuclei arises from the photodissociated surfaces of FUV-exposed giant molecular clouds (Crawford et al. 1985; Stacey et al. 1991a).

The molecular medium appears different in starburst nuclei, however. The [C II]/^{12}CO(1–0) line intensity ratio is a factor of 3–4 larger for these galaxies—close to the ratio obtained for Galactic star formation regions such as the Orion interface region (Crawford et al. 1985; Stacey et al. 1991a).[8] These large ratios are the direct result of the elevated FUV fields present in these sources (Table 3; Wolfire et al. 1989). These high FUV fields increase both the mass fraction contained in PDRs (to more than 10% in starburst nuclei) and the molecular gas excitation. The very high fields present in the Orion interface region ($\chi_{UV} \sim 10^5 \chi_0$) increase the excitation temperature for the ^{12}CO(1–0) transition to $\gtrsim$100 K (see above) much in excess of the 10–20 K observed over the bulk of the Orion molecular cloud. We therefore expect that the high-FUV fields present in starburst nuclei ($\chi_{UV} \sim 10^3 \chi_0$; Wolfire et al. 1989; Stacey et al. 1991a) may raise ^{12}CO(1–0) line excitation temperature for these sources. This may result in overestimates of the molecular gas mass if the Galactic ^{12}CO(1–0) intensity to molecular mass conversion factor is used.

[8] Note, however, that the molecular medium in starburst nuclei may *not* be constructed through a superposition of Orion interface regions—the [C II] line to far-IR continuum ratio is a factor of 10 larger for both starburst and nonstarburst galactic nuclei than it is for the Orion interface region (Table 3). The molecular medium in starburst nuclei *is* similar to a superposition of molecular clouds exposed to far-UV interstellar radiation fields $\sim 10^3 \chi_0$ (Stacey et al. 1991a).

We thank the staff and crew of the Kuiper Airborne Observatory for their excellent support. We are indebted to the referee, Hideo Matsuhara, for many constructive comments and criticisms. This work was supported in part by NASA grant NAG2-208.

REFERENCES

Bally, J., Langer, W. D., & Lui, W. 1991, ApJ, 383, 645
Beckwith, S., Persson, S. E., Neugebauer, G., & Becklin, E. E. 1978, ApJ, 223, 464
Boland, W., & de Jong, T. 1982, ApJ, 268, 110
Boreiko, R. T., Betz, A. L., & Zmuidzinas, J. 1988, ApJ, 325, L47
———. 1989, ApJ, 337, 332
Burton, M. G., Hollenbach, D. J., & Tielens, A. G. G. M. 1990, ApJ, 365, 620
Crawford, M. K., Genzel, R., Townes, C. H., & Watson, D. M. 1985, ApJ, 291, 755
Crawford, M. K., Lugten, J. B., Fitelson, W., Genzel, R., & Melnick, G. J. 1986, ApJ, 303, L57
Drain, B. T. 1978, ApJS, 36, 595
Erickson, E. F., Knacke, R. F., Tokunaga, A. T., & Haas, M. R. 1981, ApJ, 245, 148
Flower, D. R., & Launay, J. M. 1977, J. Phys, B, 10, 3673
———. 1985, MNRAS, 214, 271
Genzel, R., Poglitsch, A., & Stacey, G. J. 1988, ApJ, 333, L59
Genzel, R., Reid, M. J., Moran, J. M., & Downes, D. 1981, ApJ, 244, 884
Genzel, R., Watson, D. M., Crawford, M. K., & Townes, C. H. 1985, ApJ, 296, 766
Graf, U. U., Genzel, R., Harris, A. I., Hills, R. E., Russell, A. P. G., & Stutzki, J. 1990, ApJ, 358, L49
Gredel, R., Lepp, S., & Dalgarno, A. 1987, ApJ, 323, L137
Harris, A. I. 1986, Ph.D. thesis, Univ. California, Berkeley
———. 1988, Int. J. Infrared Millimeter Waves, 9, 231
Harris, A. I., Jaffe, D. T., Stutzki, J., & Genzel, R. 1987a, Int. J. Infrared Millimeter Waves, 8, 587
Harris, A. I., Stutzki, J., Genzel, R., Lugten, J. B., Stacey, G. J., & Jaffe, D. T. 1987b, ApJ, 322, L49
Harper, D. A. 1974, ApJ, 192, 557
Hawkins, I., & Jura, M. 1987, ApJ, 317, 926
Hildebrand, R. H., Loewenstein, R. F., Harper, D. A., Orton, G. S., Keene, J., & Whitcomb, S. E. 1985, Icarus, 64, 64
Hollenbach, D., & McKee, C. F. 1989, ApJ, 342, 306
Howe, J. E., Jaffe, D. T., Genzel, R., & Stacey, G. J. 1991, ApJ, 373, 158
Howe, J. E., Jaffe, D. T., Grossman, E. N., Wall, W. F., Mangum, J. G., & Stacey, G. J. 1992, ApJ, submitted
Jaffe, D. T., Davidson, J. A., Dragovan, M., & Hildebrand, R. H. 1984, ApJ, 284, 637
Jaffe, D. T., Genzel, R., Harris, A. I., Howe, J. E., Stacey, G. J., & Stutzki, J. 1990, ApJ, 353, 265
Jaffe, D. T., & Pankonin, V. 1978, ApJ, 226, 869
Jaquet, R., Staemmler, V., Smith, M. D., & Flower, D. 1992, J. Phys. B, 25, 285
Johansson, L. E. B., et al. 1984, A&A, 130, 227
Johnston, K. J., Palmer, P., Wilson, T. L., & Bieging, J. H. 1983, ApJ, 271, L89
Keene, J., Blake, G. A., Phillips, T. G., Huggins, P. J., & Beichman, C. 1985, ApJ, 299, 967
Koepf, G. A., Buhl, D., Chin, G., Peck, D. D., Fetterman, H. R., Clifton, B. J., & Tannenwald, P. E. 1982, ApJ, 260, 584
Kurtz, N. T., Smyers, S. D., Russell, R. W., Harwit, M., & Melnick, G. 1983, ApJ, 264, 538
Langer, W. 1976, ApJ, 206, 699
Langer, W. D., Graedel, T. E., Frerking, M. A., & Armentrout, P. B. 1984, ApJ, 277, 581
Langer, W. D., & Penzias, A. A. 1990, ApJ, 357, 477
Lugten, John B. 1987, Ph.D. thesis, Univ. California, Berkeley
Maddalena, R. J., Morris, M., Moscowitz, J., & Thaddeus, P. 1986, ApJ, 303, 375
Madden, S. C., Geis, N., Genzel, R., Herrmann, F., Jackson, J. M., Poglitsch, A., Stacey, G. J., & Townes, C. H. 1992, ApJ, submitted
Matsuhara, H., et al. 1989, ApJ, 339, L67
Melnick, G., Stacey, G. J., Viscuso, P. J., & Fuller, C. E. 1986, ApJ, 303, 638
Monteiro, T. S., & Flower, D. R. 1987, MNRAS, 228, 101
Mundy, L. G., Scoville, N. Z., Baath, L. B., Masson, C. R., & Woody, D. P. 1986, ApJ, 304, L51
Parmar, P. S., Lacy, J. H., & Achtermann, J. M. 1991, ApJ, 372, L25
Phillips, T. G., & Huggins, P. J. 1981, ApJ, 251, 533
Prasad, S. S., & Tarafdar, S. P. 1983, ApJ, 267, 603
Russell, R. W., Melnick, G. J., Gull, G. E., & Harwit, M. 1980, ApJ, 240, L99
Russell, R. W., Melnick, G. J., Smyers, S. D., Kurtz, N. T., Gosnell, T. R., Harwit, M., & Werner, M. W. 1981, ApJ, 250, L35
Schinke, R., Engel, V., Buck, U., Meyer, H., & Diercksen, G. H. F. 1985, ApJ, 299, 939
Schloerb, F. P., & Loren, R. B. 1982, in Ann. NY Acad. Sci. 395, Symp. on the Orion Nebula to Honor Henry Draper, ed. A. E. Glassgold, P. J. Huggins, & E. L. Schuking, 32
Schmid-Burgk, J., Densing, R., Krugel, E., Nett, H., Roeser, H. P., Schaefer, F., Schwaab, G., van der Wal, P., & Wattenback, R. 1989, A&A, 215, 150
Shibai, H., et al. 1991, ApJ, 374, 522
Stacey, G. J. 1985, Ph.D. thesis, Cornell Univ.
Stacey, G. J., Geis, N., Genzel, R., Lugten, J. B., Poglitsch, A., Sternberg, A., & Townes, C. H. 1991a, ApJ, 373, 423
Stacey, G. J., Kurtz, N. T., Smyers, S. D., Harwit, M., Russell, R. W., & Melnick, G. J. 1982, ApJ, 257, L37
Stacey, G. J., Smyers, S. D., Kurtz, N. T., & Harwit, M. 1983, ApJ, 265, L7
Stacey, G. J., Townes, C. H., Poglitsch, A., Madden, S. C., Jackson, J. M., Herrmann, F., Genzel, R., & Geis, N. 1991b, 382, L37
Stacey, G. J., Viscuso, P. J., Fuller, C. E., & Kurtz, N. T. 1985, ApJ, 289, 803
Stacey, G. J., et al. 1992, in preparation
Sternberg, A., & Dalgarno, A. 1989, ApJ, 338, 197
Stutzki, J., Stacey, G. J., Genzel, R., Harris, A. I., Jaffe, D. T., & Lugten, J. B. 1988, ApJ, 332, 379
Tielens, A. G. G. M., & Hollenbach, D. 1985a, ApJ, 291, 722
———. 1985b, ApJ, 291, 747
van Dishoeck, E. F., & Black, J. H. 1988, ApJ, 334, 771
Watson, D. M., Genzel, R., Townes, C. H., & Storey, J. W. V. 1985, ApJ, 298, 316
Werner, M. W. 1970, Astrophys. Lett., 6, 81
———. 1982, in Ann. NY Acad. Sci. 395, Symp. on the Orion Nebula to Honor Henry Draper, ed. A. E. Glassgold, P. J. Huggins, & E. L. Schuking, 79
Werner, M. W., Crawford, M. K., Genzel, R., Hollenbach, D. J., Townes, C. H., & Watson, D. M. 1984, ApJ, 282, L81
Werner, M. W., Gatley, I., Harper, D. A., Becklin, E. E., Loewenstein, R., Telesco, C. M., & Thronson, H. A., Jr. 1976, ApJ, 204, 420
Wilson, T. L., Serabyn, E., Henkel, C., & Walmsley, C. M. 1986, A&A, 158, L1
Wolfire, M. G., Hollenbach, D., & Tielens, A. G. G. M. 1989, ApJ, 344, 770
Wolfire, M. G., Tielens, A. G. G. M., & Hollenbach, D. 1990, ApJ, 358, 116
Wright, N., et al. 1991, ApJ, 381, 200